

Research Paper

Estimation of Metal Foam Microstructure Parameters for Maximum Sound Absorption Coefficient in Specified Frequency Band Using Particle Swarm Optimisation

Rohollah Fallah MADVARI⁽¹⁾, Mohsen Niknam SHARAK^{(2)*},
Mahsa Jahandideh TEHRANI⁽³⁾, Milad ABBASI⁽⁴⁾

⁽¹⁾ *Occupational Health Research Center, Department of Occupational Health Engineering, School of Public Health Shahid Sadoughi University of Medical Sciences Yazd, Iran*

⁽²⁾ *Department of Mechanical Engineering, University of Birjand Birjand, Iran*

*Corresponding Author e-mail: mohsen.niknam@birjand.ac.ir

⁽³⁾ *Australian Rivers Institute, Griffith University Queensland, Australia*

⁽⁴⁾ *Social Determinants of Health Research Center, Saveh University of Medical Sciences Saveh, Iran*

(received July 6, 2021; accepted January 21, 2022)

The study aims to estimate metal foam microstructure parameters for the maximum sound absorption coefficient (SAC) in the specified frequency band to obtain optimum metal foam fabrication. Lu's theory model is utilised to calculate the SAC of metallic foams that refers to three morphological parameters: porosity, pore size, and pore opening. After Lu model validation, particle swarm optimisation (PSO) is used to optimise the parameters. The optimum values are obtained at frequencies 250 to 8000 Hz, porosity of 50 to 95%, a pore size of 0.1 to 4.5 mm, and pore opening of 0.07 to 0.98 mm. The results revealed that at frequencies above 1000 Hz, the absorption efficiency increases due to changes in the porosity, pore size, and pore opening values rather than the thickness. However, for frequencies below 2000 Hz, increasing the absorption efficiency is strongly correlated with an increase in foam thickness. The PSO is successfully used to find optimum absorption conditions, the reference for absorbent fabrication, on a frequency band 250 to 8000 Hz. The outcomes will provide an efficient tool and guideline for optimum estimation of acoustic absorbents.

Keywords: porosity; pore size; pore opening; sound absorption coefficient (SAC); particle swarm optimisation (PSO).



Copyright © 2022 R.F. Madvari *et al.*
This is an open-access article distributed under the terms of the Creative Commons Attribution-ShareAlike 4.0 International (CC BY-SA 4.0 <https://creativecommons.org/licenses/by-sa/4.0/>) which permits use, distribution, and reproduction in any medium, provided that the article is properly cited, the use is non-commercial, and no modifications or adaptations are made.

1. Introduction

The World Health Organization (WHO) estimated that by 2050 over 700 million people (or one in every ten people) in the world with disabling hearing loss (WHO, 2021a). If nothing is done, the number of people with hearing loss will probably rise. Estimations have indicated that by 2050 nearly 2.5 billion people worldwide or 1 in 4 people will be living with some de-

gree of hearing loss (WHO, 2021b). WHO states that governments can expect a return of approximately \$ 16 for every \$ 1 invested in hearing care (WHO, 2021b). Measures to prevent, identify and address hearing loss are affordable and are beneficial to individuals.

Engineering controls aim to make changes in processes, machines, or equipment so that workers are less exposed to noise. For example, using mufflers, barriers, enclosures, and absorbent materials helps to reduce

noise (BIES *et al.*, 2017). In recent years metallic foams have emerged in scientific research and have been widely applied in industry and acoustics (GUAN *et al.*, 2015). The sound absorption attributes of metal foams are remarkable with the theoretical models reported in the literature (ALLARD, ATALLA, 2009; ASHBY *et al.*, 2000; ARROYO *et al.*, 2014).

Many parameters can affect the sound absorption coefficient (SAC) of aluminum foam, including porosity, pore size, pore opening, thickness, flow resistivity (GUAN *et al.*, 2015). HAN *et al.* (2003) pointed out that porous aluminum with an open cell structure, produced by the diffusion process, significantly improved sound absorption capacity compared to a close cell one. Their study showed that air movement through the attached pores affects the sound absorption capacity. Concerning that air movement is dependent on the cell structure, it is momentous to control the cell parameters for the development of porous metals with high sound absorption capacity (HAN *et al.*, 2003). Various studies have been conducted on the effect of pore size on the SAC of open cell porous metals due to the importance of cellular structure control (LU *et al.*, 2000; KUROMURA *et al.*, 2007; HAKAMADA *et al.*, 2006a; 2006b; XIE *et al.*, 2004a). Limited studies have examined optimisation of the stated parameters.

It is time consuming, costly or difficult to obtain optimal acoustic parameters in laboratory conditions. So an acoustic model is required to optimise the parameters. Such a model has been developed and provides a momentous reference for other studies on acoustic absorption materials (ZHANG, ZHU, 2016). LU *et al.* (2000) developed a model for calculating sound absorption coefficient in aluminum foam semi-open cell structures. There is a good agreement between this model and empirical measurements of sound absorption. Other researchers have confirmed the remarkable properties of this model (KUROMURA *et al.*, 2007; HAKAMADA *et al.*, 2006a; 2006b; LI *et al.*, 2011).

In recent decades, metaheuristic algorithms have gained much attention in solving complex optimisation problems. Particle Swarm Optimisation (PSO) is a commonly used metaheuristic algorithm in different fields. Swarm intelligence and information flow are the most momentous prerequisites for collaboration in this approach. When we want to create meaningful collaboration in a community, a concept called "self-organisation" and population pattern control are needed. The PSO addresses these concepts. This algorithm is one of the metaheuristic methods developed by KENNEDY and EBERHART (1995), inspired by the social behaviour of a group of birds migrating to reach an unknown destination.

Initially, this algorithm was applied to discover patterns related to the simultaneous flight of birds, sudden change of their direction, and optimal deformation of their flock. In the PSO, particles (birds) search their

destinations in the search space (KENNEDY, EBERHART, 1995; HU *et al.*, 2004). The displacement of particles in the search space is influenced by the experience and their information and neighbours' (KENNEDY, EBERHART, 1995; HU *et al.*, 2004). So the location of the particle swarm helps particle to update their position and velocity over the training process (*ibid.*). The result of modelling this social behaviour is a search process that guides particles to find an optimum solution (*ibid.*). The PSO performs based on the principle that at any given iteration, each particle adjusts its position in the search space according to the best situation it has ever been and the best place in its whole neighbourhood (*ibid.*). The PSO offers many advantages compared to other optimisation algorithms. This algorithm is suitable for nonlinear design spaces and requires less computational effort. PSO can also easily handle a variety of continuous, discrete, and numerical variables (BANSOD, MOHANTY, 2016).

In the previous studies (JAFARI *et al.*, 2020; 2021), the morphological parameters of metal foam were optimised using the local search algorithm and genetic algorithm. Using the results obtained from the PSO in this work and previous studies, readers who are looking for a suitable algorithm for making optimised metal foam can more easily choose from the proposed algorithms. In addition, if they want to present a hybrid algorithm, they can more easily understand the strengths and weaknesses of these algorithms to solve problems.

PSO is applied in this work to obtain parameter ranges of porosity (Ω), pore size (D), and pore opening (d) in a timely, precise, and efficient manner. First, the benchmarking method will be applied to perform and validate Lu's model using MATLAB software. After model validation, the PSO is implemented to optimise morphological parameters (porosity, pore size, and pore opening) in the frequencies ranging from 250 to 8000 Hz. The optimisation process is designed for the maximum absorption coefficient.

2. Methods

The main objective of this study is to optimise the parameters affecting the sound absorption coefficient. In this section, we introduce and validate the Lu model. Then, we discuss the PSO algorithm in detail.

2.1. Lu model

A schematic model of porous foam is shown in Fig. 1. LU *et al.* (2000) proposed a model based on experimental and theoretical studies for aluminum foams with semi-open cells in sound absorption surveys. This model emphasises the relationship between sound absorption and morphological parameters such as pore size, pore opening, and porosity. According to the Lu

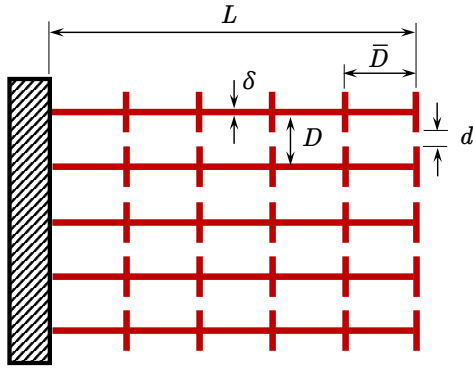


Fig. 1. Schematic model of metallic foam.

model, the acoustic impedance of the air inside a cell (Z_D) is obtained from Eq. (1) (LU *et al.*, 2000):

$$Z_D = -i\rho_0 c_0 \cot\left(\frac{2\pi f \bar{D}}{c_0}\right), \quad (1)$$

where $\bar{D} = 0.806D$. The acoustic impedance of the open cell (Z_0) is as follows:

$$Z_0 = R_0 + iM_0, \quad (2)$$

where the special acoustic resistance (R_0) and the open cell reactance among the pores (M_0) are as follow:

$$R_0 = \frac{32\eta\delta}{d^2} \left(\sqrt{\frac{1+\beta^2}{32}} + \sqrt{\frac{\beta d}{4\delta}} \right), \quad (3)$$

$$M_0 = 2\pi f \rho_0 \delta \left(1 + \frac{1}{\sqrt{(9+\beta^2)/32 + \bar{d}/\delta}} \right),$$

where $\bar{d} = 0.85d$. Parameters Z_D , z_0 , R_0 , and M_0 are obtained in [Pa·s/m]. In Eqs (1) to (3), $\rho_0 = 1.184 \text{ kg/m}^3$ is the air density, $\eta = 1.849 \cdot 10^{-5} \text{ Pa}\cdot\text{s}$ is the air dynamic (absolute) viscosity, and $c_0 = 346.5 \text{ m/s}$ is the sound velocity in the air at 25°C. D [m] is the pore size, d [m] is the pore opening, f [Hz] is the frequency of the sound wave, and $i^2 = -1$.

The cell wall thickness (δ [m]) and dimensionless parameter β are as follow:

$$\delta = \frac{(1-\Omega)D}{3.55-6I^2}, \quad (4)$$

$$\beta = \frac{\sqrt{\Omega\rho_0\eta}d}{2},$$

where $I = d/D$ is the identical pore connectivity of a material, and Ω is the porosity [%]. The acoustic impedance (Z_1) is obtained from Eq. (5):

$$Z_1 = z_0 + Z_D, \quad (5)$$

where $z_0 = (0.909D/d)^2 Z_0$ is the ratio of the specific sound impedance of the cell cavity.

When the number of cells in the direction of sound distribution (n) is greater than 1, the acoustic impedance (Z_n) is as follows (LU *et al.*, 2000):

$$Z_n = R_n + iM_n = z_0 + \frac{Z_D Z_{n-1}}{Z_D + Z_{n-1}}. \quad (6)$$

Finally, the sound absorption coefficient (SAC) of the metal foam is as follows:

$$\alpha = \rho_0 c_0 \left(\frac{4R_n}{(\rho_0 c_0 + R_n)^2 + (M_n)^2} \right). \quad (7)$$

In Eqs (1) to (7), porosity (Ω), pore size (D), and pore opening (d) are the only independent parameters. If we want to maximise the sound absorption coefficient, we must determine these parameters optimally. In this study, the range of these parameters is according to previous studies that achieved satisfactory agreement between analytical and experimental results from the Lu model (LU *et al.*, 2000; HAKAMADA *et al.*, 2006a; LI ET AL., 2011; MENG *et al.*, 2014). These ranges are as follow:

$$50 \leq \Omega \leq 95\%, \quad 0.1 \leq D \leq 3.5 \text{ mm}, \quad (8)$$

$$0.01 \leq d \leq 0.4 \text{ mm}.$$

2.2. Verification

Governing equations are validated to ensure that code is correctly performed in MATLAB software. The results of this study are compared with (LU *et al.*, 2000) and the measured values. The sample 'd' of this reference with the thickness of 20 mm is investigated and Table 1 shows its properties.

Table 1. Properties of sample 'd' according to (LU *et al.*, 2000).

Sample	Bulk density [g/cm ³]	Porosity [%]	Pore size [mm]	Pore opening [mm]
'd'	0.932	65.47	1.06	0.400

To investigate the prediction model, Table 2 shows the comparison between the current predictions, the experimental data, and Lu experimental model. According to Table 2, the solved example is following the Lu model confirming the written code. The next step is to conduct the optimisation using the PSO algorithm.

2.3. Particle swarm optimisation (PSO)

Particle swarm optimisation (PSO) is a population-based optimisation algorithm in which each individual is considered as a particle and each population consists of a number of such particles (HAMERLY, ELKAN, 2002; PAN *et al.*, 2006). In the PSO, the problem solving space is considered as the search space, and each

Table 2. Comparison of the results of this study with the predicted and measured results of LU *et al.* (2000).

Frequency [Hz]	200	300	500	700	900	1100	1400	1700
Experiment	0.1716	0.1231	0.1306	0.1455	0.1978	0.2612	0.4067	0.5560
LU <i>et al.</i> (2000)	0.0007	0.0012	0.0352	0.0787	0.1481	0.2624	0.4850	0.7275
Error [%]	99.6	99.03	73.05	45.91	25.13	0.46	19.25	30.84
Present work	0.0038	0.0092	0.0287	0.0629	0.1155	0.1905	0.3473	0.5343
Error [%]	97.79	92.53	78.02	56.77	41.61	27.07	14.61	3.90

location in the search space is a problem-related solution. Particles work together to find the best solution in the search space (solution space) (HAMERLY, ELKAN, 2002; PAN *et al.*, 2006). Each particle moves in accordance with its velocity. The movement of each particle in each iteration is calculated by the following formula (HAMERLY, ELKAN, 2002; PAN *et al.*, 2006; NATH *et al.*, 2018):

$$P_i(t+1) = P_i(t) + V_i(t+1), \quad (9)$$

$$V_i(t+1) = wV_i(t) + c_1r_1(Pbest_i(t) - P_i(t)) + c_2r_2(Gbest(t) - P_i(t)), \quad (10)$$

where $P_i(t)$ and $V_i(t)$ are the position and the velocity of i -th particle at iteration t , respectively. $Pbest_i(t)$ is particle's best known position found by the i -th particle, $Gbest(t)$ is the best position known to the swarm, w is the inertia weight that gives a ratio of the previous velocity, c_1 and c_2 are the acceleration coefficients that determine the effect of each particle's best position and the best global position, and $r_1, r_2 \in [0, 1]$ are random numbers (CURA, 2009; CAMPANA *et al.*, 2013). The procedure of the PSO algorithm is shown in Fig. 2. There are several types of stopping criteria that can be specified in the PSO:

- 1) reaching an acceptable limit of response,
- 2) passing the number of iterations or specified time,
- 3) passing the number of iterations or specified time without observing a specific improvement in the result,
- 4) checking a certain number of responses.

2.4. PSO adjustment parameters

In this study, after validating the code written by Lu study in MATLAB software, the authors applied the concept of constriction coefficients according to the study of CLERC and KENNEDY (2002). Accordingly, two arbitrary positive real numbers ϕ_1 and ϕ_2 must be chosen to be greater than four, which means:

$$\phi \equiv \phi_1 + \phi_2 > 4. \quad (11)$$

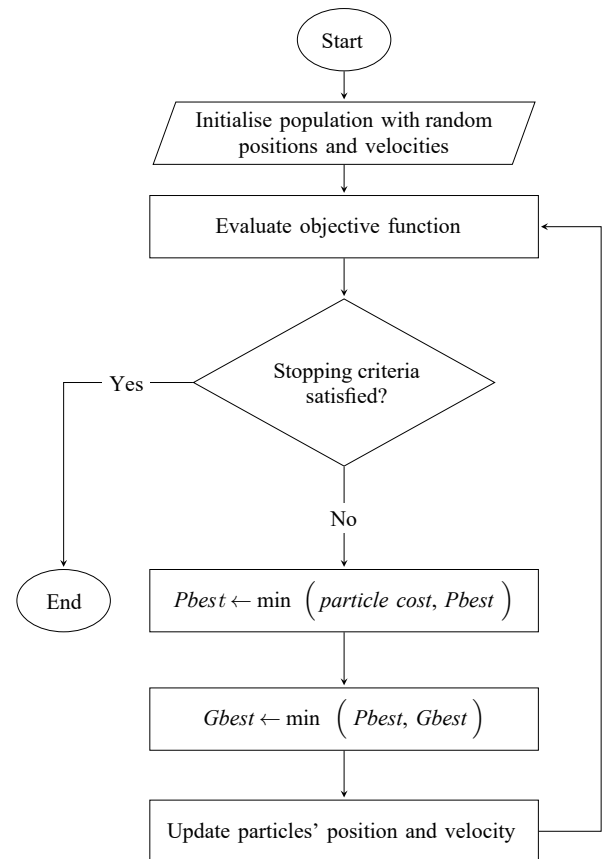


Fig. 2. Structure of particle swarm optimisation algorithm.

Parameter χ is defined as:

$$\chi = \frac{2}{\phi - 2 + \sqrt{\phi^2 - 4\phi}}. \quad (12)$$

Then, the PSO adjustment parameters will be as follows:

$$w = \chi, \quad c_1 = \chi\phi_1, \quad c_2 = \chi\phi_2. \quad (13)$$

CLERC and KENNEDY'S (2002) analysis showed that $\phi_1 = \phi_2 = 2.05$ are the optimum values. The population size is not very sensitive to problem, and the prevalent selection is 20–50 (WANG *et al.*, 2018), so we used 30 particles to cover the entire domain. We also set the maximum number of iterations to 150. Convergence plot analysis (see Fig. 3 in next section) confirms that

150 iterations are reasonable for achieving the optimal solution. To increase the algorithm accuracy in this study, the particle movement velocity in the PSO algorithm is restricted using the following equation (DEL VALLE *et al.*, 2008; CLERC, 2010):

$$|V_{\max}| = 0.1(X_{\max} - X_{\min}), \quad (14)$$

where X is the vector of variables, and in the present work defined as follows:

$$X = [d, D, \Omega]^T \quad (15)$$

and superscript T presents the transpose of the vector. The maximum value of the SAC will be equal to one. Therefore, in this research, the objective function is defined as follows:

$$F = \min(\sqrt{(1 - \alpha)^2}). \quad (16)$$

3. Results

The convergence plots of the PSO algorithm for each thickness at the frequency of 6000 Hz are indicated in Fig. 3. Considering the convergence plot (Fig. 3), it is clear that the value of the response does not change from one iteration to the next; therefore, the number of iterations selected is appropriate for obtaining the optimal response.

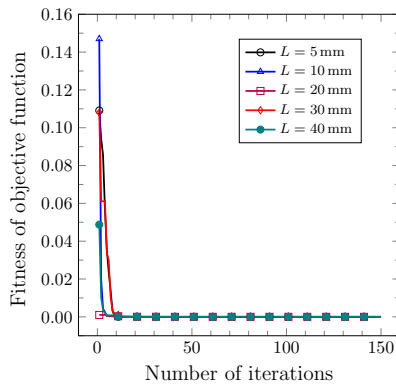


Fig. 3. Convergence plot of the PSO algorithm for different thicknesses at frequency 6000 Hz.

The results of the estimated (optimum) parameters using the PSO are presented in Figs 4 to 8 for thicknesses of 5, 10, 20, 30, and 40 mm, respectively. In the PSO, three physical parameters are optimised at different frequencies. In Figs 4 to 8, the left hand plots indicate the optimisation results for a specific defined range of parameters, Eq. (8), and the right hand plots show the optimisation results for free range of the parameters.

Figure 4 shows the optimum parameters for the maximum absorption coefficient at a thickness of 5 mm for each frequency. Figure 4 indicates the sound absorption coefficients of 0.9 and 1 at frequencies of 2000

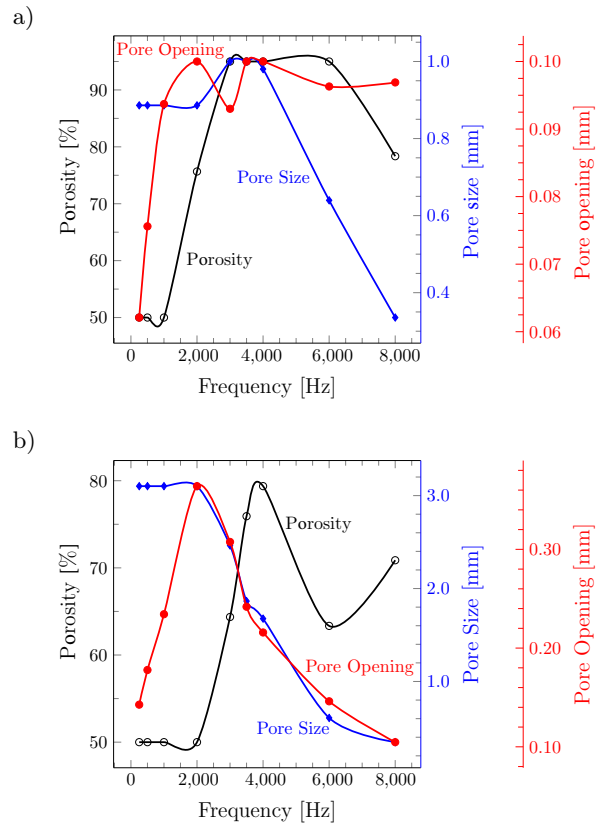


Fig. 4. Estimated parameters using the PSO for thickness of 5 mm for: a) defined ranges, Eq. (8), and b) free ranges.

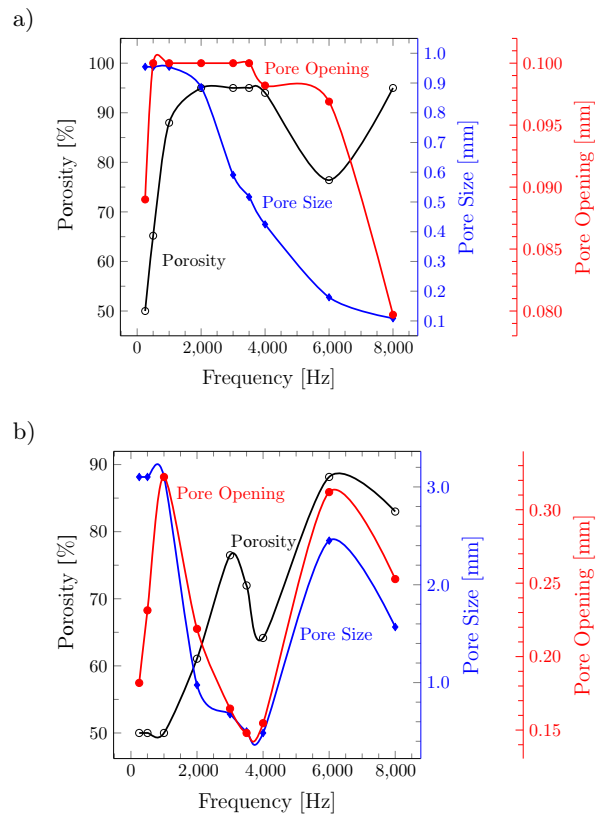


Fig. 5. Estimated parameters using the PSO for thickness of 10 mm for: a) defined ranges, Eq. (8), and b) free ranges.

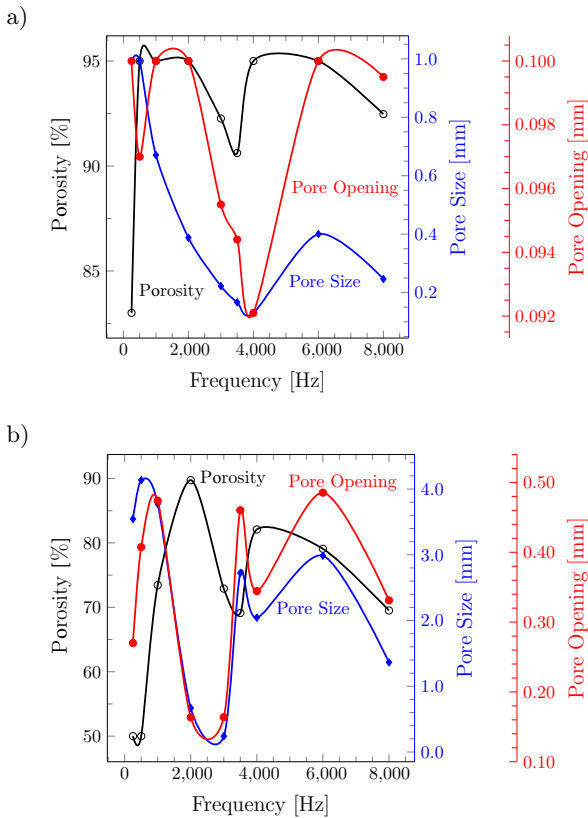


Fig. 6. Estimated parameters using the PSO for thickness of 20 mm for: a) defined ranges, Eq. (8), and b) free ranges.

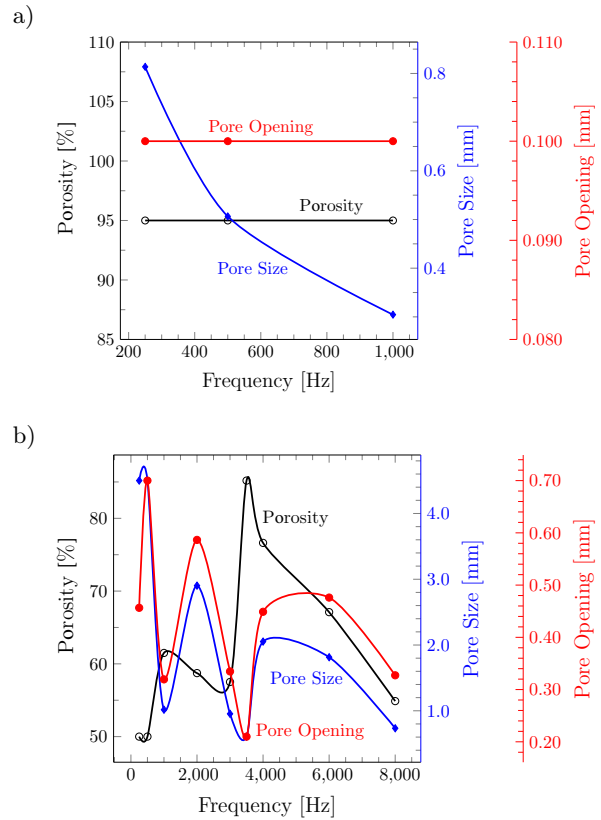


Fig. 8. Estimated parameters using the PSO for thickness of 40 mm for: a) defined ranges, Eq. (8), and b) free ranges.

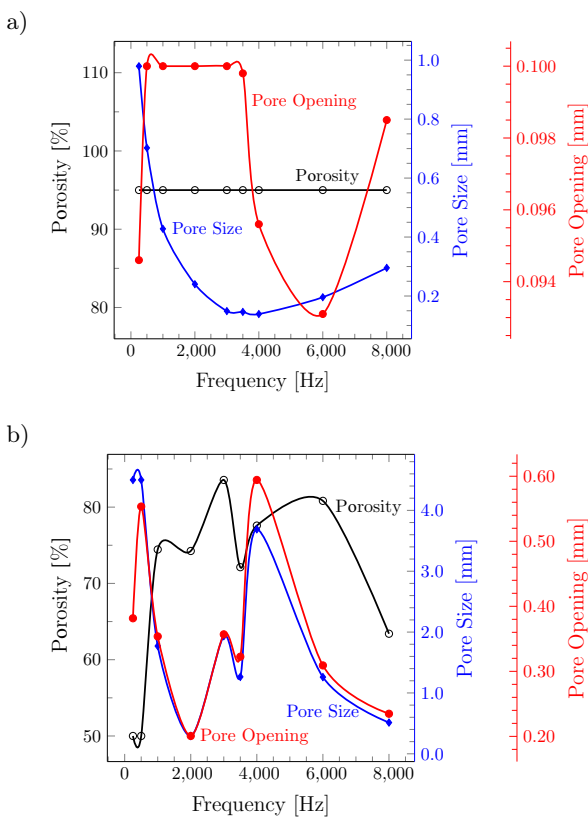


Fig. 7. Estimated parameters using the PSO for thickness of 30 mm for: a) defined ranges, Eq. (8), and b) free ranges.

to 8000 Hz, porosity between 50 to 95%, pore size of 0.33 to 3.1 mm, and pore opening of 0.09 to 0.36 mm. Furthermore, at low frequencies of 250 to 1000 Hz, the absorption coefficient does not increase since the main limitation is low thickness. Therefore, optimum absorption coefficient is obtained only at high frequencies. According to the results, frequency increase leads to pore size and pore opening decreases, whereas such frequency increase has no impact on porosity.

Figure 5 represents the results of the optimum parameters at a thickness of 10 mm for each frequency. Figure 5 reveals the sound absorption coefficient of almost one at frequencies between 2000 to 8000 Hz, porosity between 61 to 95%, pore size between 0.1 to 1.4 mm, and pore opening of 0.07–0.31 mm. According to the results, the optimum parameters with respect to the frequency do not have a definite order, and no general rule can be driven to describe them. In other words, pore size, porosity, pore opening, and sound absorption parameters do not rely on frequency changes.

Figure 6 shows the optimal value of the absorption coefficient parameters in the thickness of 20 mm. The results indicate the absorption coefficient of almost one at frequencies between 1000–8000 Hz, porosity between 69–95%, pore size between 0.1–3.7 mm, and pore opening between 0.09–0.48 mm. According

Table 3. Optimised sound absorption coefficient at different thicknesses for each frequency using the PSO.

Frequency [Hz]	250	500	1000	2000	3000	3500	4000	6000	8000
$L = 5$ mm	0.0747	0.1645	0.4205	0.9795	1.0000	1.0000	1.0000	1.0000	1.0000
$L = 10$ mm	0.1227	0.2818	0.7267	1.0000	1.0000	1.0000	1.0000	1.0000	1.0000
$L = 20$ mm	0.2341	0.6391	1.0000	1.0000	1.0000	1.0000	1.0000	1.0000	1.0000
$L = 30$ mm	0.3729	0.8972	1.0000	1.0000	1.0000	1.0000	1.0000	1.0000	1.0000
$L = 30$ mm	0.5138	0.9995	1.0000	1.0000	1.0000	1.0000	1.0000	1.0000	1.0000

to Fig. 6, similar to Fig. 5, pore size, porosity, pore opening, and sound absorption parameters do not rely on frequency changes.

Figure 6 shows the results of the optimal value of the parameters for the thickness of 30 mm. This figure represents the absorption coefficients of about one at frequencies of 1000 to 8000 Hz, porosity between 63 to 95%, pore size of 0.1 to 3.6 mm, and pore opening of 0.09 to 0.98 mm. The optimum parameters with respect to the frequency do not have a definite order.

Figure 8 reveals the sound absorption of one at frequencies of 500 to 8000 Hz, porosity of 50 to 95%, pore size of 0.3 to 4.5 mm, and pore opening between 0.1 to 0.7 mm. According to Fig. 8, there is no significant correlation between sound absorption coefficient and the pore size, porosity, and pore opening values under frequency increase. However, at low frequency (500–1000 Hz), there is an increase in the SAC of 5 mm thickness. Therefore, at low frequencies, the thickness increase can potentially lead to the SAC increases.

Table 3 represents the value of optimised absorption coefficient at different thicknesses for each frequency. As shown in Table 3, at frequencies below 1000 Hz, increase in the SAC corresponds to the panel thickness increase. However, for frequencies above 1000 Hz, conditions can be found for each thickness (i.e., D , d , and Ω) in which the maximum sound absorption value is achieved. It can be also observed that at frequencies above 1000 Hz, no increase in thickness is needed to increase the absorbent efficiency (increase in sound absorption rate), and thickness increase can be obtained simply by changing the porosity, pore size, and pore opening values.

4. Discussion

In this study, the PSO method was used to obtain the optimum pore size, pore opening size, porosity, and thickness for the metal foam absorbent, in accordance with Lu model and developed coding in MATLAB software. Comparison of the coding results with those of Lu's research confirmed the validity of Lu theoretical model in evaluating the sound absorption performance of porous metal foam. LU model is reliable for simulating sound absorption in porous metals with bottleneck structures and can be used as a tool to optimise porous

structures using porosity and pore size as variables. According to the optimisation results of this study, generally the frequency, porosity, pore size, and pore opening parameters to obtain the highest absorption coefficient (almost one) range between 250–8000 Hz, 50–95%, 0.1–4.5 mm, and 0.07–0.98 mm, respectively.

In this study, it was found that there is no specific correlation between porosity and absorption coefficient under frequency changes, and LU *et al.* (2000) also showed that there was no obvious relationship between sound absorption and porosity. The results showed that at each frequency and thickness, the maximum absorption coefficient porosity had a specific value, whereas previous studies stated that the SAC increases by porosity increase (XIE *et al.*, 2004a; 2004b; LU *et al.*, 1999; KUROMURA *et al.*, 2007).

According to JIN *et al.* (2015), as the foam porosity increases, the sound absorption coefficient also increases, which is inconsistent with the present study. According to the results of this study, it was found that for each maximum absorption coefficient, the optimum pore size is needed, and its range was between 0.1–4.5 mm in our research.

WANG and LU (1999) stated that the optimal pore size for best sound absorption was about 0.1 mm. NAVACERRADA *et al.* (2013) investigated aluminum foam with a pore size of 0.5, 1, and 2 mm. Aluminum foam with a pore diameter of 0.5 mm showed the highest absorption capacity, which is in accordance with the optimisation range of the pore size in the present study (0.1–4.5 mm). RAUT *et al.* (2016) reported that as the foam thickness increases, the maximum sound absorption shifts to lower frequencies, which is in line with the current study. They stated that by decreasing the pore opening size, the maximum sound absorption shifts to lower frequencies, which is not in line with the present study. Moreover, a fixed value cannot be defined.

LI *et al.* (2011) concluded that the sound absorption coefficient increases by increasing the number of pore openings per single area or by decreasing the pore diameter in the range of 0.3–0.4 mm, which is in the optimisation range of the present study (0.07–0.98 mm). The results showed that at 5 mm thickness, the pore size is decreasing with increased frequency for maximum absorption coefficient. According to pre-

vious results, the SAC increases by decreasing pore size (ZHANG, ZHU, 2016; HAN *et al.*, 2003; XIE *et al.*, 2004).

Kuromura's study (KUROMURA *et al.*, 2007) stated that the sound absorption coefficient varies with pore size changes, which is in line with the results of this study. In (HAKAMADA *et al.*, 2006), sample 'B', with the smallest pore size ranging (212–300 μm) had the highest SAC, which is in range of parameters obtained from the optimisation of this study. In some studies, pore diameters were reported in the range of 0.5 to 2 mm (LU *et al.*, 2000; WANG, LU, 1999), which are still within the optimisation range of this study (0.1 to 4.5 mm). In the study of WANG and LU (1999), it was proposed the pore size optimum for the highest sound absorption capacity of approximately 100 μm using a computational method; however, in this study the amount of pore size varies in different frequencies and thicknesses. LI *et al.* (2011) stated that there was no specific correlation between pore size and the SAC of aluminum foam with spherical cells, which is in accordance with the current study. HAKAMADA and KUROMURA (2006a) stated that the lack of apparent correlation between pore size and the sound absorption coefficient is due to significant diaphragm effects, which is in line with the results of this study. This clearly demonstrates the importance of controlling the pore opening size for the ability to absorb sound (HAKAMADA *et al.*, 2006b). In this study, pore opening size parameter varies at different values of frequency and thickness. Recently, the importance of pore opening size in air flow resistivity to porous metals has been emphasized (HAKAMADA *et al.*, 2006a; DESPOIS, MORTENSEN, 2005). Therefore, it has been suggested that the pore opening size strongly affects the sound absorption behaviour and the control of the aperture size is crucial for achieving the SAC (HAKAMADA *et al.*, 2006a). Hence, the pore opening size requires a certain range as well as optimisation for each thickness and frequency. In the present study, the amount of pore opening was between 0.07–0.98 mm, which had no correlation with the absorption coefficient at different thicknesses and frequencies.

According to Figs 4 to 8, it can be seen that at low frequencies, increasing thickness from 5 to 40 mm leads to the sound absorption coefficient increase from 0.16 to 0.99 and from 0.42 to 1 at frequency of 500 Hz and 1000 Hz, respectively. The SAC raised by increasing sample thickness in the low frequency ranges between 500–1000 Hz, which is similar to that of Hakamada's study (2006b). Moreover, WANG *et al.* (2011) reported that at low frequencies, the absorption coefficient of sound is low for thin sample with open porosity of more than 90%. In this study, as the frequency or thickness of the sample increases, the sound absorption also increases significantly. HAN *et al.* (2003) reported that increasing the sample thickness also increases the

air flow resistivity and thus increases the absorption capacity. LI *et al.* (2011) stated that as the sample thickness increases, the absorption peak shifts to lower frequencies. They also noted that the effect of sample thickness on sound absorption is understandable due to the long propagation distance in relatively thick samples, which results in increased acoustic wave interaction with the pore walls (*ibid.*). Furthermore, it is evident that at frequencies above 1000 Hz, the thickness does not need to be increased in order to increase the absorption efficiency (increase in sound absorption rate), and this can be achieved only by changing the porosity, pore size, and pore opening values. In this study it was found that the factors of porosity, pore size, and pore opening are essential for optimisation. Studies have shown that porous metal foam using optimum morphology shows better acoustic absorption behaviours than non-optimum samples at different frequencies.

5. Conclusion

Changing porosity, pore size, and pore opening is an efficient strategy for sound absorption spectrum engineering of open cellular foam. Lu model is reliable for simulating the sound absorption in porous metals with bottleneck structures. In this study, the PSO algorithm was used to optimise the three parameters affecting Lu model absorption coefficient for metal foam. Comparing the coding results of this study with those of Lu model, we confirmed the validity of the theoretical model in evaluating the sound absorption performance of porous metal foam. At frequencies above 1000 Hz, absorption coefficient of almost one can be achieved by optimising the porosity, pore size, and pore opening; however, at low frequencies, the thickness has a significant effect on increasing the absorption coefficient. According to the optimisation results of this study, to obtain the highest absorption coefficient (approximately one), the range of frequencies, porosity, pore size, and pore opening parameters need to be between 250–8000 Hz, 50–95%, 0.1–4.5 mm, 0.07–0.98, respectively. Interestingly, at low frequencies between 500 and 1000 Hz, the thickness of the absorption coefficient increased by 40 mm compared to the thickness of 5 mm. In this study, it was found that no fixed value can be defined for pore size, porosity, and pore opening. Additionally, there was no specific correlation between the stated parameters and absorption coefficient under changed frequency. Therefore, the values of sound absorption coefficient varied at each frequency and thickness, which emphasizes the importance of applying optimisation in this research. Sound absorption raised by increasing thickness of the metal foam absorbent at low frequencies. The method presented in this study can be a reliable reference and guide for future studies to optimise the micro-structural param-

ters and to increase the sound absorption coefficient at each frequency, and can also help in optimised metal foam fabrication. As a suggestion for future research work, other models such as the Johnson-Champoux-Allard-Lafarge-Pride (JCALP) model can be used for optimisation and compared with this study.

Acknowledgements

This work was supported by the Shahid Sadoughi University of Medical Sciences with project code 9476 and ethics code: IR.SSU.SPH.REC.1400.062.

References

1. ALLARD J., ATALLA N. (2009), *Propagation of Sound in Porous Media: Modelling Sound Absorbing Materials*, 2nd ed., John Wiley & Sons, doi: 10.1002/9780470747339.
2. ARROYO E., RAYESS N., WEAVER J. (2014), Enhanced sound absorption of aluminum foam by the diffuse addition of elastomeric rubbers, *The Journal of the Acoustical Society of America*, **135**(4): 2375–2375, doi: 10.1121/1.4877838.
3. ASHBY M.F., EVANS A.G., FLECK N.A., GIBSON J.L., HUTCHINSON J.W., WADLEY H.N.G. [Eds] (2000), *Metal Foams: A Design Guide*, Butterworth-Heinemann: Burlington, doi: 10.1016/B978-0-7506-7219-1.X5000-4.
4. BANSOD P.V., MOHANTY A. (2016), Inverse acoustical characterization of natural jute sound absorbing material by the particle swarm optimization method, *Applied Acoustics*, **112**: 41–52, doi: 10.1016/j.apacoust.2016.05.011.
5. BIES D.A., HANSEN C.H., HOWARD C.Q. (2017), *Engineering Noise Control*, CRC Press: Boca Raton, doi: 10.1201/9781351228152.
6. CAMPANA E.F., DIEZ M., FASANO G., PERI D. (2013), Initial particles position for PSO, in bound constrained optimization, [in:] *Advances in Swarm Intelligence. ICSI 2013. Lecture Notes in Computer Science*, Tan Y., Shi Y., Mo H. [Eds], Vol. 7928, pp. 112–119, Springer-Verlag: Berlin, Heidelberg, doi: 10.1007/978-3-642-38703-6_13.
7. CLERC M. (2010), *Particle Swarm Optimization*, John Wiley & Sons, doi: 10.1002/9780470612163.
8. CLERC M., KENNEDY J. (2002), The particle swarm-explosion, stability, and convergence in a multidimensional complex space, *IEEE transactions on Evolutionary Computation*, **6**(1): 58–73, doi: 10.1109/4235.985692.
9. CURA T. (2009), Particle swarm optimization approach to portfolio optimization, *Nonlinear Analysis: Real World Applications*, **10**(4): 2396–2406, doi: 10.1016/j.nonrwa.2008.04.023.
10. DEL VALLE Y., VENAYAGAMOORTHY G.K., MOHAGHEGHI S., HERNANDEZ J.-C., HARLEY R.G. (2008), Particle swarm optimization: basic concepts, variants and applications in power systems, *IEEE Transactions on Evolutionary Computation*, **12**(2): 171–195, doi: 10.1109/TEVC.2007.896686.
11. DESPOIS J.-F., MORTENSEN A. (2005), Permeability of open-pore microcellular materials, *Acta Materialia*, **53**(5): 1381–1388, doi: 10.1016/j.actamat.2004.11.031.
12. GUAN D., WU J.H., WU J., LI J., ZHAO W. (2015), Acoustic performance of aluminum foams with semi-open cells, *Applied Acoustics*, **87**: 103–108, doi: 10.1016/j.apacoust.2014.06.016.
13. HAKAMADA M., KUROMURA T., CHEN Y., KUSUDA H., MABUCHI M. (2006a), High sound absorption of porous aluminum fabricated by spacer method, *Applied Physics Letters*, **88**(25): 254106, doi: 10.1063/1.2216104.
14. HAKAMADA M., KUROMURA T., CHEN Y., KUSUDA H., MABUCHI M. (2006b), Sound absorption characteristics of porous aluminum fabricated by spacer method, *Journal of Applied Physics*, **100**(11): 114908, doi: 10.1063/1.2390543.
15. HAMERLY G., ELKAN C. (2002), Alternatives to the k-means algorithm that find better clusterings, [in:] *Proceedings of the Eleventh International Conference on Information and Knowledge Management*, pp. 600–607, doi: 10.1145/584792.584890.
16. HAN F., SEIFFERT G., ZHAO Y., GIBBS B. (2003), Acoustic absorption behaviour of an open-celled aluminium foam, *Journal of Physics D: Applied Physics*, **36**(3): 294, doi: 10.1088/0022-3727/36/3/312.
17. HU X., SHI Y., EBERHART R. (2004), Recent advances in particle swarm, [in:] *Proceedings of the 2004 Congress on Evolutionary Computation (IEEE Cat. No. 04TH8753)*, Vol. 1, pp. 90–97, doi: 10.1109/CEC.2004.1330842.
18. JAFARI M.J., KHAVANIN A., EBADZADEH T., FAZLALI M., SHARAK M.N., MADVARI R.F. (2020), Optimization of the morphological parameters of a metal foam for the highest sound absorption coefficient using local search algorithm, *Archives of Acoustics*, **45**(3): 487–497, doi: 10.24425/aoa.2020.134066.
19. JAFARI M.J., MADVARI R.F., SHARAK M.N., EBADZADEH T. (2021), Improving the morphological parameters of aluminum foam for maximum sound absorption coefficient using genetic algorithm, *Sound & Vibration*, **55**(2): 117–130, doi: 10.32604/sv.2021.09729.
20. JIN W. et al. (2015), Sound absorption characteristics of aluminum foams treated by plasma electrolytic oxidation, *Materials*, **8**(11): 7511–7518, doi: 10.3390/ma8115395.
21. KENNEDY J., EBERHART R. (1995), Particle swarm optimization, [in:] *Proceedings of ICNN'95 – International*

- Conference on Neural Networks*, Vol. 4, pp. 1942–1948, doi: 10.1109/ICNN.1995.488968.
22. KUROMURA T., HAKAMADA M., CHEN Y., KUSUDA H., MABUCHI M. (2007), Sound absorption behavior of porous al produced by spacer method, [in:] *Advanced Materials Research*, Vol. 15, pp. 422–427, Trans Tech Publications Ltd, doi: 10.4028/www.scientific.net/amr.15-17.422.
 23. LI Y., WANG X., WANG X., REN Y., HAN F., WEN C. (2011), Sound absorption characteristics of aluminum foam with spherical cells, *Journal of Applied Physics*, **110**(11): 113525, doi: 10.1063/1.3665216.
 24. LU T.J., CHEN F., HE D. (2000), Sound absorption of cellular metals with semiopen cells, *The Journal of the Acoustical Society of America*, **108**(4): 1697–1709, doi: 10.1121/1.1286812.
 25. LU T.J., HESS A., ASHBY M. (1999), Sound absorption in metallic foams, *Journal of Applied Physics*, **85**(11): 7528–7539, doi: 10.1063/1.370550.
 26. MENG H., XIN F., LU T.J. (2014), Sound absorption optimization of graded semi-open cellular metals by adopting the genetic algorithm method, *Journal of Vibration and Acoustics*, **136**(6): 061007, doi: 10.1115/1.4028377.
 27. NATH S., SING J.K., SARKAR S.K. (2018), Performance comparison of PSO and its new variants in the context of VLSI global routing, [in:] *Particle Swarm Optimization with Applications*, Erdoğan P. [Ed.], Ch. 5, IntechOpen: Rijeka, doi: 10.5772/intechopen.72811.
 28. NAVACERRADA M., FERNÁNDEZ P., DÍAZ C., PEDREIRO A. (2013), Thermal and acoustic properties of aluminium foams manufactured by the infiltration process, *Applied Acoustics*, **74**(4): 496–501, doi: 10.1016/j.apacoust.2012.10.006.
 29. PAN H., WANG L., LIU B. (2006), Particle swarm optimization for function optimization in noisy environment, *Applied Mathematics and Computation*, **181**(2): 908–919, doi: 10.1016/j.amc.2006.01.066.
 30. RAUT S.V., KANTHALE V., KOTHAVALA B. (2016), Review on application of aluminum foam in sound absorption technology, *International Journal of Current Engineering and Technology*, Special Issue 4: 178–181, 10.14741/Ijcet/22774106/spl.4.2016.36.
 31. WANG D., TAN D., LIU L. (2018), Particle swarm optimization algorithm: an overview, *Soft Computing*, **22**(2): 387–408, doi: 10.1007/s00500-016-2474-6.
 32. WANG X., LU T.J. (1999), Optimized acoustic properties of cellular solids, *The Journal of the Acoustical Society of America*, **106**(2): 756–765, doi: 10.1121/1.427094.
 33. WANG X.F., WANG X.F., WEI X., HAN F.S., WANG X.L. (2011), Sound absorption of open celled aluminium foam fabricated by investment casting method, *Materials Science and Technology*, **27**(4): 800–804, doi: 10.1179/026708309X12506934374047.
 34. World Health Organization (2021a), *Deafness and hearing loss*, <https://www.who.int/news-room/fact-sheets/detail/deafness-and-hearing-loss>.
 35. World Health Organization (2021b), *WHO: 1 in 4 people projected to have hearing problems by 2050*, <https://www.who.int/news/item/02-03-2021-who-1-in-4-people-projected-to-have-hearing-problems-by-2050>.
 36. XIE Z., IKEDA T., OKUDA Y., NAKAJIMA H. (2004a), Sound absorption characteristics of lotus-type porous copper fabricated by unidirectional solidification, *Materials Science and Engineering: A*, **386**(1–2): 390–395, doi: 10.1016/j.msea.2004.07.058.
 37. XIE Z., IKEDA T., OKUDA Y., NAKAJIMA H. (2004b), Characteristics of sound absorption in lotus-type porous magnesium, *Japanese Journal of Applied Physics*, **43**(10R): 7315, doi: 10.1143/jjap.43.7315.
 38. ZHANG B., ZHU J. (2016), Inverse methods of determining the acoustical parameters of porous sound absorbing metallic materials, *Proceedings of Meetings on Acoustics 22ICA*, **28**(1): 015006, doi: 10.1121/2.0000329.